

Lawrence Berkeley National Laboratory

Recent Work

Title

C12(x,xn)C11 AND Al27(x, x2pn)Na24 CROSS SECTIONS AT HIGH ENERGIES

Permalink

<https://escholarship.org/uc/item/3p00n89s>

Authors

Birnbaum, Wallace
Crandall, Walter E.
Millburn, George P.
et al.

Publication Date

1954-11-01

A
UCRL 2756

UNCLASSIFIED

UNIVERSITY OF
CALIFORNIA

*Radiation
Laboratory*

TWO-WEEK LOAN COPY

*This is a Library Circulating Copy
which may be borrowed for two weeks.
For a personal retention copy, call
Tech. Info. Division, Ext. 5545*

BERKELEY, CALIFORNIA

DISCLAIMER

This document was prepared as an account of work sponsored by the United States Government. While this document is believed to contain correct information, neither the United States Government nor any agency thereof, nor the Regents of the University of California, nor any of their employees, makes any warranty, express or implied, or assumes any legal responsibility for the accuracy, completeness, or usefulness of any information, apparatus, product, or process disclosed, or represents that its use would not infringe privately owned rights. Reference herein to any specific commercial product, process, or service by its trade name, trademark, manufacturer, or otherwise, does not necessarily constitute or imply its endorsement, recommendation, or favoring by the United States Government or any agency thereof, or the Regents of the University of California. The views and opinions of authors expressed herein do not necessarily state or reflect those of the United States Government or any agency thereof or the Regents of the University of California.

UNIVERSITY OF CALIFORNIA
Radiation Laboratory
Berkeley, California

Contract No. W-7405-eng-48

$C^{12} (x, xn) C^{11}$ AND $Al^{27} (x, x2pn) Na^{24}$ CROSS SECTIONS
AT HIGH ENERGIES

Wallace Birnbaum, Walter E. Crandall, George P. Millburn,
and Robert V. Pyle

November 1, 1954

$C^{12}(x, xn)C^{11}$ AND $Al^{27}(x, x2pn)Na^{24}$ CROSS SECTIONS
AT HIGH ENERGIES

Contents

Abstract 3

I. Introduction 4

II. Experimental Procedure

 A. Beam Characteristics and Monitoring 5

 B. Degradation of Particle Energy 5

 C. Foils 6

 D. 4π Proportional Counter 7

III. Results

 A. Energy Dependence of Cross Sections 8

 B. Absolute Values of the Cross Sections 9

 C. End-Window Counter Measurements 11

IV. Summary and Conclusions 12

Acknowledgments 13

References 16

$C^{12} (x, xn) C^{11}$ AND $Al^{27} (x, x2pn) Na^{24}$ CROSS SECTIONS
AT HIGH ENERGIES

Wallace Birnbaum, * Walter E. Crandall, George P. Millburn,
and Robert V. Pyle

Radiation Laboratory, Department of Physics
University of California, Berkeley, California

November 1, 1954

ABSTRACT

The $C^{12} (x, xn) C^{11}$ and $Al^{27} (x, x2pn) Na^{24}$ cross sections were measured for protons (105 to 350 Mev), deuterons (85 to 190 Mev), and alpha particles (380 Mev) by using a 4π β counter to determine the absolute disintegration rate and measuring the incident flux with a Faraday cup. The absolute value of the $C^{12} (p, pn) C^{11}$ excitation function was found to be 20 percent lower than the value previously published for these energies, and was found to be constant between 200 and 350 Mev. The new value of this reaction cross section removes some of the discrepancies between p-p scattering cross sections measured elsewhere and those measured at Berkeley, and affects other experiments that use the reaction as a proton flux monitor. The other cross sections are in reasonable agreement with values determined by comparable methods.

The relative excitation functions for $C^{12} (d, dn) C^{11}$ and $C^{12} (He^3, He^3 n) C^{11}$ reactions were also measured by a stacked-foil technique using end-window counters. These were normalized to absolute values from the 4π counter data for deuterons.

*Now at the University of California Radiation Laboratory, Livermore, California.

$C^{12} (x, xn) C^{11}$ AND $Al^{27} (x, x2pn) Na^{24}$ CROSS SECTIONS
AT HIGH ENERGIES

Wallace Birnbaum,* Walter E. Crandall, George P. Millburn,
and Robert V. Pyle

Radiation Laboratory, Department of Physics
University of California, Berkeley, California

November 1, 1954

I. INTRODUCTION

Absolute cross sections for reactions producing C^{11} and Na^{24} from bombardment of C^{12} and Al^{27} with high-energy particles have been determined for protons of 105 to 350 Mev, deuterons of 85 to 190 Mev, and alpha particles of 380 Mev using the external beams of the 184-inch cyclotron. Many of the excitation functions have been determined previously, some by essentially the same technique used in this experiment,¹⁻⁵ but because of the importance of these reaction cross sections for beam monitoring⁶⁻⁸ it was decided to redetermine the absolute values separately. An important feature of the experiment was the nearly concurrent measurement of all the cross sections, which should insure high accuracy of the ratios.

The method involved absolute determination of the number of particles impinging on the targets by use of a Faraday cup, and absolute determination of the disintegration rate by use of a 4π , constant-flow, methane proportional counter calibrated against a similar instrument at the National Bureau of Standards.**

Besides a desire to redetermine the absolute cross sections in view of recent advances in absolute β counting, an incentive for the experiment was the discrepancy in the shape of the $C^{12} (p, pn) C^{11}$ excitation function near 350 Mev as reported by two different groups.^{1,2} Two different methods of degrading the proton energy were used to explore the reasons for the discrepancy. The same technique was applied to the $C^{12} (d, dn) C^{11}$ excitation function near the maximum available energy (190 Mev). The $C^{12} (\alpha, \alpha n) C^{11}$ and

*Now at the University of California Radiation Laboratory, Livermore, California.

**We are indebted to Dr. H. H. Seliger of the Radioactivity Section of the National Bureau of Standards for his assistance in providing us with sources previously calibrated in their 4π β counter.

$Al^{27}(x, x2pn)Na^{24}$ reaction cross sections were measured only for the maximum particle energies.

In an experiment which preceded the bulk of the work being reported, the relative excitation functions for the $C^{12}(d, dn)C^{11}$ and $C^{12}(He^3, He^3n)C^{11}$ reactions were measured by a stacked-foil technique. An end-window counter was used in these experiments and the results were normalized from the 4π counter data for deuterons. Although the precision of these measurements is low compared with the other cross sections, the values are included for completeness.

The following discussions relate only to the techniques and procedures used in the 4π counter experiments; discussion of the end-window counter data is reserved for the end of the paper.

II. EXPERIMENTAL PROCEDURE

A. Beam Characteristics and Monitoring

A plan view of the cyclotron is shown in Fig. 1. Most of the measurements were made with the scattered external beam which emerges from the magnetic deflectors, passes over the proton probe cart, through the premagnet collimator, through the steering magnet, and then through the 48-inch collimator and into the experimental area (cave). All of the beams used were monoenergetic to within less than one percent.

The beam was monitored by a Faraday cup.¹ The signal from the cup was led to one of several low-leakage Fast condensers which had been calibrated against a similar condenser measured by the National Bureau of Standards to within 0.1 percent.* Measurements made with different condensers showed excellent agreement. The voltage on the condenser was measured by a 100 percent inverse-feedback integrating electrometer and a Speedomax recorder, which were calibrated against a Rubicon potentiometer to within 0.1 percent. The uncertainty in the beam monitoring is believed to be less than 1 percent.

B. Degradation of Particle Energy

Carbon absorbers placed in front of the target foils in the path of the beam were used to degrade the incident energy. The particle current that

*We are indebted to A. H. Scott and C. Peterson of the Electricity Division of the National Bureau of Standards for assistance in obtaining the calibration.

emerges from the absorbers is contaminated with relatively low-energy particles, which were thought to be the cause of the discrepancies mentioned above in the shape of the $C^{12}(p, pn)C^{11}$ excitation function near 350 Mev.² Absorbers were placed in two positions in an attempt to measure the effect of the secondary particles. Position A was directly before the Faraday cup, so that the particles emerged from the absorber and passed through the target foils into the Faraday cup. This was essentially the technique used by Aamodt et al¹ to degrade the proton energy. Because the $C^{12}(x, xn)C^{11}$ cross section increases for energies lower than those used in this experiment (see Fig. 2), the effect of low-energy secondary particles on the excitation function is magnified in relation to their number. Absorbers were also placed in position B, which was on the proton probe cart (Fig. 1) in the path of the scattered beam. The collimators and steering magnet then provided a good energy selector, and low-energy charged particles were no longer present in the beam entering the cave. Absorbers were also placed at position A in these experiments to obtain further energy degradation and to study the effect of the secondary particles as a function of the incident-particle energy.

Actually, several absorbers were used at position A and target foils were placed at various depths. The Faraday cup then measured the current through the last foil. To determine the current (primary plus charged secondary particles) that passed through the other foils in the absorber, separate measurements were made with an ionization chamber in front of the absorber. The same absorbers used above were then in turn inserted between the chamber and the Faraday cup to measure the fraction, I/I_0 , of the beam that passed through foils placed at the various depths in the absorber. This technique gives the total particle current at each foil position to an accuracy comparable with the direct measurement of the incident current, since measurements at 350 Mev with no absorber in the beam path were consistent with these results.

In analogy to the geometries defined in scattering experiments, measurements made with the absorbers at position A are referred to as "poor geometry" measurements, while those at position B are referred to as "good geometry" measurements.

C. Foils

The carbon foils were made of polystyrene, $(CH)_n$, and were 1 or 1-1/4 in. in diameter. The thicknesses varied from 1 to 15 mils. Some of the foils were coated with very thin layers (of the order of 100 angstroms) of silver in

order to test the effect of nonconducting samples on the efficiency of the 4π proportional counter as described below. The aluminum foils were of the same diameters and 5 and 10 mils thick. In an auxiliary experiment, aluminum foils of thicknesses down to $1/4$ mil were activated in order to extrapolate the results to zero foil thicknesses, and foils varying from $1/4$ to $1-1/2$ in. in diameter were activated in order to check the efficiency of the counter.

Each of the target foils represents a slice of a "thick" slab of the foil material. "Guard" foils of 5 mils thickness were placed between foils of different elements and between foils and absorbers in order to insure against recoil loss and capture.^{9,10} In addition, several foils were usually stacked at each absorber depth, and no variation in apparent cross section was observed in these foils.

The beam diameter was $1/2$ in. when the 1-inch-diameter foils were used, and $3/4$ in. when the $1-1/4$ -inch-diameter foils were used. The foils were large enough to intercept all the beam, including the multiply scattered portion. This was shown by inserting photographic film at each absorber depth; the blackening was always confined to an area less than that of the foils.

The foils were weighed and measured to an accuracy of about 0.1 percent (except for the thin aluminum foils in the auxiliary experiment, which were weighed to an accuracy of about 1 percent). The foils were counted for 3 or more half lives; the C^{11} activity fitted best a 20.4-min. half life, and the Na^{24} a 15.1-hr. half life.

D. 4π Proportional Counter

The target foils were counted in a 4π constant-flow methane proportional counter.¹¹ The poorest plateaus obtained had slopes of about $1/3$ percent per hundred volts over a 300-volt range. No discriminator plateaus were taken because the discriminator was fixed internally at a point above the noise level. The operation of such a counter has been described by Seliger and Cavallo.¹¹

Since the field is low at the sample position when nonconducting foils are counted,¹¹ several polystyrene foils were coated with silver to a thickness of approximately 100 angstroms (measured by the comparative light transmission of coated and uncoated foils). There was never any significant difference between the determinations of the cross section with an uncoated foil and those with a coated foil, which indicates that essentially all of the β particles here are energetic enough to escape the low-field region. This problem did not enter when aluminum foils were used.

Long-lived, β -active isotopes mounted on thin foils were used to check the performance of the counter during the period of the experiments.

In order to check the efficiency of the 4π counter against a suitable standard, three sources calibrated by the National Bureau of Standards were obtained.* Two were Tl^{204} sources and one was a $\text{Sr}^{90}\text{-Y}^{90}$ source. The sources were sandwiched between 0.2 mg/cm of aluminum leaf to prevent source losses, and the NBS calibration was made after sandwiching. The ratios of the counting rates in our counter compared with those in the NBS counter were 0.99, 1.00, and 1.01; we therefore believe our counter to be 100 ± 1 percent as efficient as the NBS counter, which is at least 99 percent efficient.¹³

III. RESULTS

A. Energy Dependence of Cross Sections

The measurements of the $\text{C}^{12}(x, xn)\text{C}^{11}$ cross sections as a function of energy showed a significant dependence on the position of the absorber in relation to the target foil. Measurements made in "poor geometry" (position A) consistently gave apparent cross sections about 7 percent higher than those measured in "good geometry" (position B). This dependence can be ascribed to the charged and uncharged secondary particles that leave the absorber. (A crude calculation of the effects agreed very well with the empirical corrections.)

Figure 3 shows the apparent cross section as a function of energy for protons. Four measurements are shown for three different incident beam energies (the incident beam energy was varied by placing absorbers in position B, and the variation with energy was determined by placing absorbers in position A). All the curves show the dip found in earlier experiments;¹ but it seems certain that the true variation of the cross section with energy is more accurately represented by the straight line drawn through the first points on each curve. The ratio of the apparent cross section as a function of absorber thickness is shown in Fig. 4. The end points of the curves in Fig. 3 were normalized to 1.000, and the ratios of the other points were found for each curve separately and averaged to give Fig. 4; in the averaging the lowest-energy point was ignored since the cross section begins here to show some significant energy variation. The conclusion drawn from Fig. 4 is that the secondary particles increase

*Courtesy of Dr. H. H. Seliger, NBS.

the observed cross section in a constant ratio for absorbers greater than a given thickness. The effect of the secondaries does not continue to increase as the absorber thickness increases because

- (1) the low-energy secondary particles are scattered, and a fraction, which increases with absorber thickness, does not pass through the foil;
- (2) the relatively low energies of the charged secondary particles mean that they are removed by ionization loss within a short distance from their creation; and
- (3) the secondary particles are emitted with an angular distribution so that a large fraction of those formed in the front of the absorber miss the foil.

The results of these measurements would seem to remove the discrepancy mentioned in the introduction in the shape of the excitation function, and would require that the excitation function reported in Reference 1 be corrected for energies below the maximum beam energy.

Similar behavior is exhibited by the $C^{12}(d, dn)C^{11}$ excitation function, although the details are different because deuteron and proton interactions give different spectra and distributions for the secondary particles.

The excitation function for $C^{12}(\alpha, \alpha n)C^{11}$ was not measured, but somewhat similar behavior probably should be expected.

B. Absolute Values of the Cross Sections

The absolute cross sections determined in this experiment are listed in Table I. The proton cross sections are averages of all the data at each energy after corrections have been made for

- (1) foil thickness as listed in Table II and shown in Figs. 5 and 6;
- (2) secondary particle contributions, by multiplying the measured values by 1/1.07 for cross sections determined with the absorbers in position A; and
- (3) the number of particles passing through the foil, as explained in Sec. IIB.

Corrections 1 and 3 were also applied to the deuteron data. The corrections for secondary-particle contribution for deuterons is somewhat more uncertain than that for protons, because the absorbers were relatively thick compared with the range. However, cross sections for 1/2-in. carbon absorber in position A were decreased by the ratio 1/1.04, and those for greater thicknesses by the ratio 1/1.08. The correction may be significantly in error for the lower deuteron energies.

The $C^{12}(\alpha, \alpha n)C^{11}$ cross section at 380 Mev is 12 ± 6 percent higher than the value found by Lindner and Osborne.³ No explanation for the difference is apparent; but the quoted uncertainties in their value are large enough so that the difference could be statistical.

Independent absolute values of the $C^{12}(d, dn)C^{11}$ cross section have not been published, so no comparison of our results is possible. The excitation function is shown in Fig. 7, which includes the data from the end-window counter experiments described below.

The $C^{12}(p, pn)C^{11}$ cross section at 350 Mev is 32.9 ± 1.1 mb, compared with the absolute value of 41.2 ± 4.6 mb reported earlier.¹ (We have changed the quoted probably error to a standard error by dividing by 0.6745 in order to conform with our practice.) The discrepancy is believed to reflect the increased accuracy of absolute β counting since the time of earlier measurements.

The absolute value of the excitation function reported in Reference 1 should be reduced in the ratio $32.9/41.2 = 0.799$ for 350-Mev protons, and in addition, the results for energies just below 350 Mev should be reduced by $1/1.07$ (or a total of $0.799/1.07 = 0.747$). The excitation function is shown in Fig. 2.

The results of readjusting the $C^{12}(p, pn)C^{11}$ cross section will be far-reaching, because of the widespread use of the reaction for beam monitors at high energies.⁶⁻⁸ For example, the p-p scattering cross sections measured at 240 Mev by Oxley et al.⁸ should certainly be modified. Even though they intercalibrated their counter with a beta standard used by Aamodt et al, the revised shape of the excitation function requires at least a 41/49 reduction in their values (to 4.05 ± 0.32 mb/sterad); the revised value agrees within experimental uncertainties with the values of Chamberlain et al at 250 Mev (3.6 ± 0.2 mb/sterad).¹²

The p-p scattering cross sections measured by Birge et al⁸ for 105- and 75-Mev protons may be reduced directly by the ratio $41.2/32.9$ (to 4.3 and 5.3 mb/sterad, respectively), because their beta-counter calibration was independent of other experimenters. The revised values are in agreement with the Berkeley measurements.¹²

The results of Cassels et al⁸ for the p-p scattering cross sections at 146 Mev were measured by using two methods to calibrate their beam monitor. The one of concern to us used the $C^{12}(p, pn)C^{11}$ reaction with a cross section of 56.9 ± 6.5 mb at 142 Mev; this gave a value of 4.61 ± 0.55 mb/sterad for

the p-p cross section, which should be reduced by 42/57 to 3.40 ± 0.40 mb/sterad. Their values that are based on a photographic emulsion calibration remain high compared with other measurements.

If the cross section for $\text{Al}^{27}(\text{p}, 3\text{pn})\text{Na}^{24}$ reported by Belmont and Miller⁷ is readjusted on the basis of our $\text{C}^{12}(\text{p}, \text{pn})\text{C}^{11}$ cross section, it agrees very well with other quoted values. (Their value becomes 11.6 mb.)

Recently Rosenfeld et al¹³ have redetermined the $\text{C}^{12}(\text{p}, \text{pn})\text{C}^{11}$ cross section at 460 Mev, and quote 33 mb as their best value, in excellent agreement with our results. Also, recent measurements at energies up to 2.9 Bev tend to confirm our value.¹⁴

The $\text{Al}^{27}(\text{x}, \text{x}2\text{pn})\text{Na}^{24}$ cross sections were measured for 350-Mev protons, 190-Mev deuterons, and 380-Mev alpha particles. The foil thicknesses were 5 and 10 mils, and the cross sections obtained were extrapolated to zero thickness from the results of an auxiliary experiment shown in Fig. 6. The absolute cross sections obtained are given in Table I and compared with measurements by other experimenters.^{3, 4, 5} The agreement is generally satisfactory, although our values tend to be systematically high.

The errors quoted in Table I are standard errors compounded from statistical errors of counting, errors in extrapolating to zero foil thickness (2 percent), errors in correcting for the secondary-particle effects (2 percent), errors from absolute beam monitoring (1 percent), and errors in the efficiency of the β counter (1 percent). Thus the statistical errors were compounded with an error of about 3 percent, which is an estimate of the uncertainty in the absolute values of the cross sections. The energies were computed from the Range-Energy Tables of Aron et al¹⁵ and rounded to the nearest 5 Mev.

C. End-Window Counter Measurements

The stacked-foil technique was used to measure the relative excitation functions of deuterons and He^3 particles for the $\text{C}^{12}(\text{x}, \text{xn})\text{C}^{11}$ reaction. Graphite foils 1-11/16 in. in diameter and 1/8 and 1/16 in. thick were placed between guard foils and inserted at various depths in uranium absorbers. Near the end of the range, the carbon foils were inserted consecutively. The incident-particle current was measured by an ionization chamber and the current through each foil determined from charge-attenuation curves measured with a Faraday cup.¹⁶

The foils were counted in an end-window β counter with a 3.5-mg/cm² window. The counter and its use in connection with these experiments are described more fully in a paper by Schecter et al.¹⁷ No activity other than the

20.4-minute C^{11} was observed; the foils were counted for several half lives. Corrections were applied for counter dead time, C^{11} decay, C^{11} decay during the length of the bombardment, and geometry differences (found empirically).

The excitation curve for deuterons was normalized to the high-energy point from 4π counter data, and the low-energy cross sections were corrected for secondary particles as in Sec. IIB. The range of the deuterons was determined for a similar stack and the energies were computed from the tables of Aron et al.¹⁵ Uncertainties in the range point cause the large energy uncertainties for low energies; the horizontal lines in Fig. 7 represent an estimate of the uncertainty in placement of the midpoint, and do not represent merely the spread (due to range straggling) of energies that pass through the foil.

The excitation function for He^3 particles shown in Fig. 8 was normalized on the basis of the deuteron data, because both curves were measured at the same time. The techniques and corrections were the same for both cases; for the cross sections shown in Fig. 8, a constant correction of 1/1.08 was applied to the data for energies lower than the maximum. The errors on the points are unsymmetrical because it is felt that such a correction for secondary-particle effects is very likely incorrect for incident He^3 particles. The inelastic and stripping cross sections for He^3 are approximately equal to those for deuterons,¹⁶ but the stripped secondaries have ranges greater than the residual range of the He^3 particle.¹⁶ Thus the effects of the secondary particles probably do not level off to a constant value as quickly as they do for protons and deuterons whose secondaries have ranges shorter than the residual range of the primary particle. Caution should be exercised when using the data of Fig. 8, for the measured shape of the excitation function is very likely incorrect. The cross section is constant within experimental error for energies greater than 80 Mev.

Measurements of the He^3 excitation function were not repeated with the technique of Secs. III A and B because it was felt that in this energy region the reaction was not likely to be useful as a monitor.

IV. SUMMARY AND CONCLUSIONS

In addition to obtaining absolute values of the cross sections, we have measured the ratios of the various reaction cross sections with a good degree of accuracy, certainly to less than 3 percent. In addition we have shown that

the $C^{12}(x, xn)C^{11}$ excitation functions are actually fairly constant at and near the maximum energies of the charged-particles beams available at Berkeley; earlier measurements that indicated a sharp dip near the maximum energy failed to take into proper account the effect of secondary particles produced in the attenuators.

The absolute value of the $C^{12}(p, pn)C^{11}$ cross section at 350 Mev is significantly lower than that reported earlier,¹ and the difference is believed to be due to the increased accuracy of absolute β -counting that has been achieved in the last few years. Readjustment of the excitation function on the basis of our results leads to improved agreement between the p-p scattering cross sections measured at Berkeley and those measured elsewhere⁸ using the $C^{12}(p, pn)C^{11}$ reaction to monitor the proton beam. The reported results of other experiments will be affected by the readjustment of the excitation function; a partial list of such experiments is given in References 6 to 8.

ACKNOWLEDGMENTS

The authors are happy to acknowledge the support and assistance of Dr. Chester M. Van Atta. We also wish to thank Frank L. Adelman, John Ise, Jr., Larry Schecter, and Marian N. Whitehead and Messrs. Donald A. Hicks and Robert M. Main for assistance in collecting data, and the cyclotron crew under the direction of James Vale for helpful cooperation. This research was sponsored by the Atomic Energy Commission.

Table I
 Absolute Reaction Cross Sections
 (4 π Counter Data Only)

	Particle Energy Mev	"Geometry"	Cross Section
A. $C^{12}(p, pn)C^{11}$	350 \pm 5	good	32.9 \pm 1.1
	320 \pm 5	good	32.4 \pm 0.9
	325 \pm 5	poor	32.7 \pm 1.1
	295 \pm 5	good	33.3 \pm 1.0
	295 \pm 5	poor	31.9 \pm 2.2
	270 \pm 5	poor	32.5 \pm 1.3
	240 \pm 5	poor	33.0 \pm 2.1
	205 \pm 5	poor	33.1 \pm 1.7
	170 \pm 5	poor	36.1 \pm 1.5
B. $C^{12}(d, dn)C^{11}$	190 \pm 5	good	56.0 \pm 1.4
	180 \pm 5	good	55.6 \pm 1.4
	180 \pm 5	poor	55.3 \pm 2.2
	160 \pm 5	good	55.9 \pm 2.1
	160 \pm 5	poor	55.3 \pm 2.3
	145 \pm 5	poor	55.1 \pm 2.4
	130 \pm 5	poor	56.1 \pm 2.2
	105 \pm 5	poor	54.8 \pm 2.3
85 \pm 5	poor	52.0 \pm 2.5	
C. $C^{12}(\alpha, \alpha n)C^{11}$	380 \pm 5	good	53.9 \pm 1.4
	380 \pm 5	good	48 \pm 3 (a)
D. $Al^{27}(p, 3pn)Na^{24}$	350 \pm 5	good	11.5 \pm 0.5
			10.2 \pm 0.2(c)
E. $Al^{27}(d, 302n)Na^{24}$	190 \pm 5	good	24.1 \pm 1.0
	190 \pm 5	good	22 \pm 2 (b)
F. $Al^{27}(\alpha, 4p3n)Na^{24}$	380 \pm 5	good	25.3 \pm 1.0
	380 \pm 5	good	23.4 \pm ? (a)

(a) See Ref. 3

(b) See Ref. 5

(c) See Ref. 4

Note: All errors are standard errors of a single measurement (not the mean), and include estimated uncertainties due to possible systematic effects. See text.

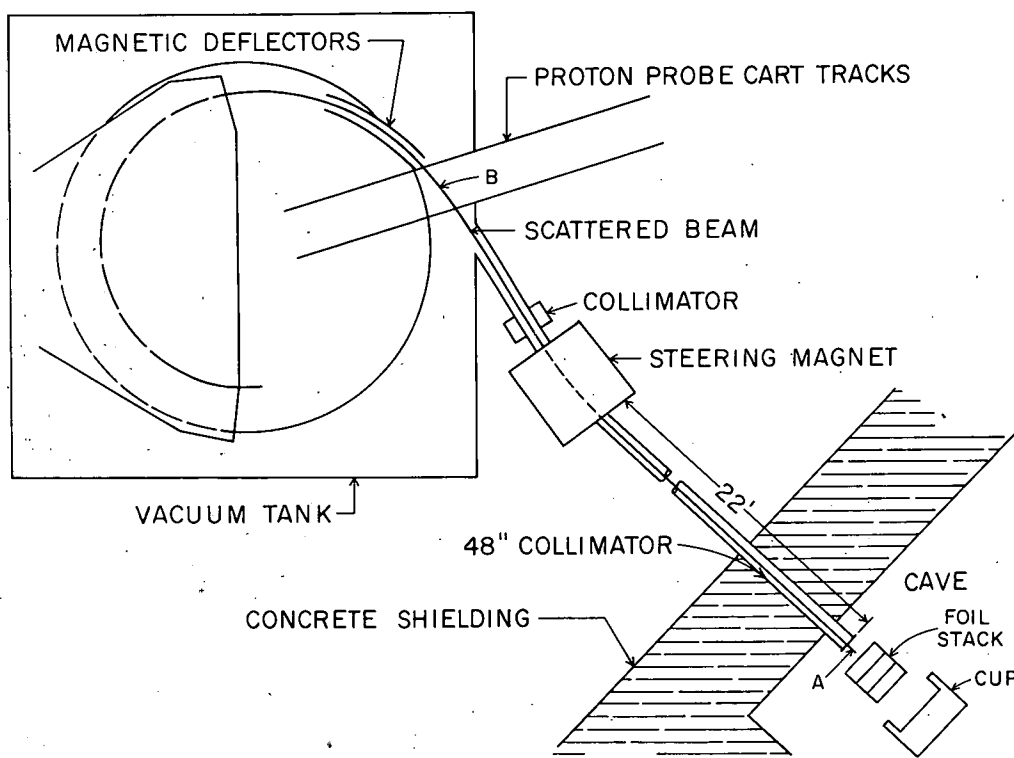
Table II

Factors to Correct Counting Rates from Thick Foils to Zero Foil Thickness

	Foil Thickness (mils)	Correction Factor
A. C ¹¹ activity, polystyrene foils	1	1.001 ± 0.015
	2	1.003 ± 0.015
	3	1.006 ± 0.015
	5	1.052 ± 0.015
	15	1.257 ± 0.024
B. Na ²⁴ activity, aluminum foils	0.25	1.000 ± 0.044
	0.50	1.013 ± 0.044
	1	1.019 ± 0.038
	2	1.067 ± 0.034
	3	1.085 ± 0.033
	5	1.139 ± 0.036
	10	1.345 ± 0.044

REFERENCES

1. R. Aamodt, V. Peterson and R. Phillips, Phys. Rev. 88, 739 (1952); W. W. Chupp and E. M. McMillan, Phys. Rev. 72, 873 (1947).
2. S. D. Warshaw, R. A. Swanson and A. H. Rosenfeld, Phys. Rev. 95, 649(A) (1954).
3. M. Lindner and R. N. Osborne, Phys. Rev. 91, 1501 and 342 (1953).
4. P. C. Stevenson, H. G. Hicks and R. L. Folger, to be published in the Physical Review.
5. R. E. Batzel, W. W. T. Crane and G. D. O'Kelley, Phys. Rev. 91, 939 (1953).
6. L. Marquez, Phys. Rev. 88, 225 (1952).
7. E. Belmont and J. M. Miller, Phys. Rev. 95, 1554 (1954).
8. J. W. Meadows, Phys. Rev. 91, 885 (1953); R. W. Birge, U. E. Kruse and N. F. Ramsey, Phys. Rev. 83, 274 (1951); C. L. Oxley and R. D. Shamberger, Phys. Rev. 85, 416 (1952); O. A. Towler and C. L. Oxley, Phys. Rev. 78, 326 (1950) and Phys. Rev. 84, 1262 (1951); K. Strauch and J. A. Hoffman, Phys. Rev. 86, 563 (1952) and Phys. Rev. 90, 449 (1953); J. W. Meadows and R. B. Holt, Phys. Rev. 83, 47 and 1257 (1951); J. B. Cassels, T. G. Pickavance and G. H. Stafford, Proc. Roy. Soc. (London) 214, 262 (1952).
9. R. E. Batzel and G. T. Seaborg, Phys. Rev. 82, 607 (1951).
10. S. Fung and I. Perlman, Phys. Rev. 87, 623 (1952).
11. H. H. Seliger and L. Cavallo, NBS J. Research 47, 41 (1951); also H. H. Seliger and A. Schwebel, Nucleonics 12, 54 (July, 1954).
12. O. Chamberlain, E. Segrè, and C. Wiegand, Phys. Rev. 83, 923 (1951).
13. A. H. Rosenfeld, private communication.
14. R. F. Wolfgang and G. Friedlander, Phys. Rev. 96, 190 (1954).
15. W. A. Aron, B. G. Hoffman and F. C. Williams, AECU-663.
16. G. P. Millburn, W. Birnbaum, W. E. Crandall, and L. Schecter, Phys. Rev. 95, 1268 (1954) and unpublished data.
17. L. Schecter, W. E. Crandall, G. P. Millburn and J. Ise, Jr., to be published in the Physical Review.



MU-8413

Fig. 1 Plan view of the cyclotron showing the path of the scattered beam. Absorbers for the "good geometry" experiments were placed on the proton probe cart and interposed in the scattered beam; the steering magnet current was then adjusted so that only particles of the proper energy entered the cave.

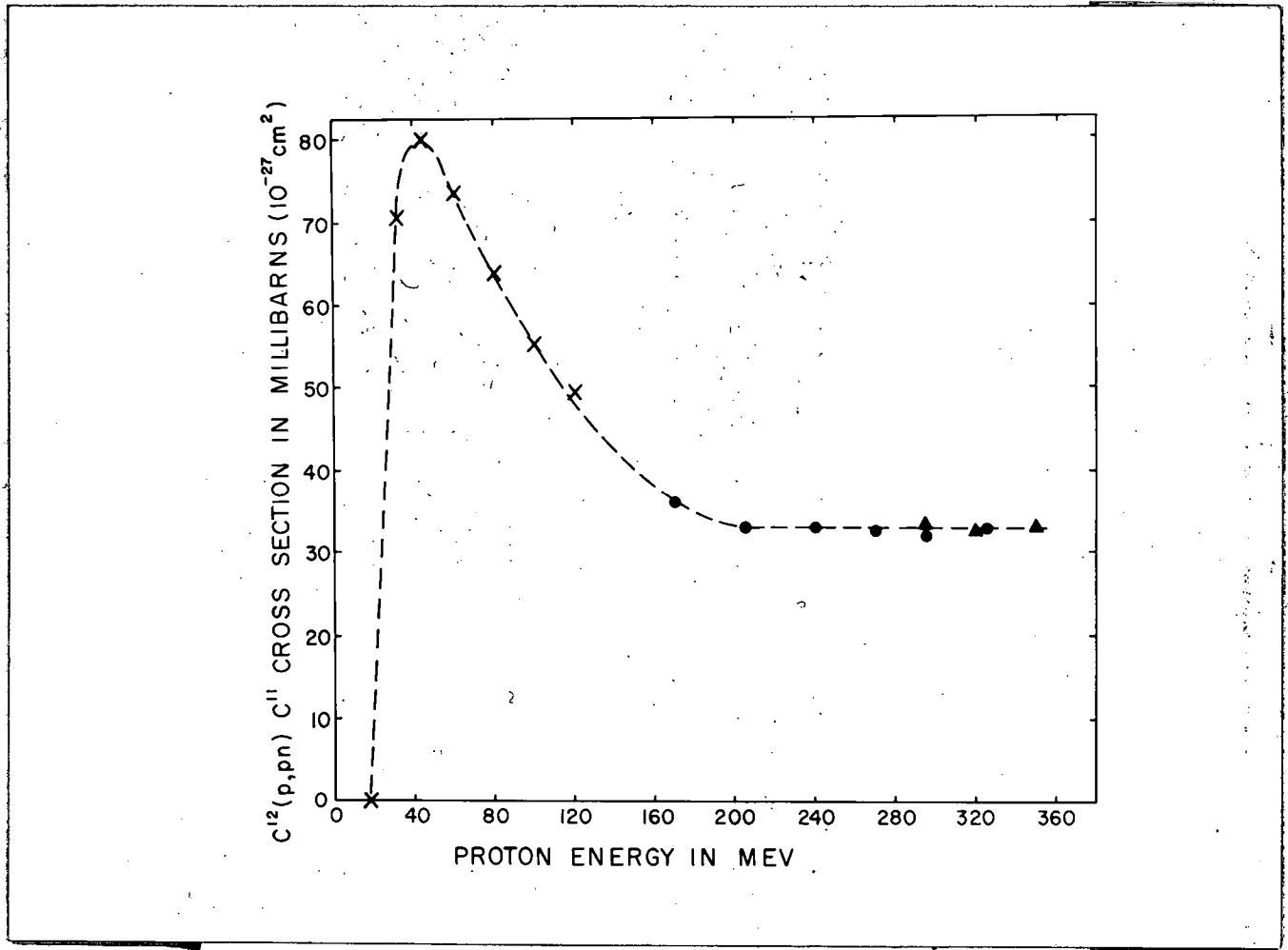


Fig. 2 The excitation function for the $C^{12}(p, pn)C^{11}$ reaction is plotted as a function of the proton energy. The triangles are "good geometry" measurements, and the dots are "poor geometry" measurements corrected as described in the text. The crosses are from the data of reference 1 normalized to 32.9 mb. at 350 Mev.

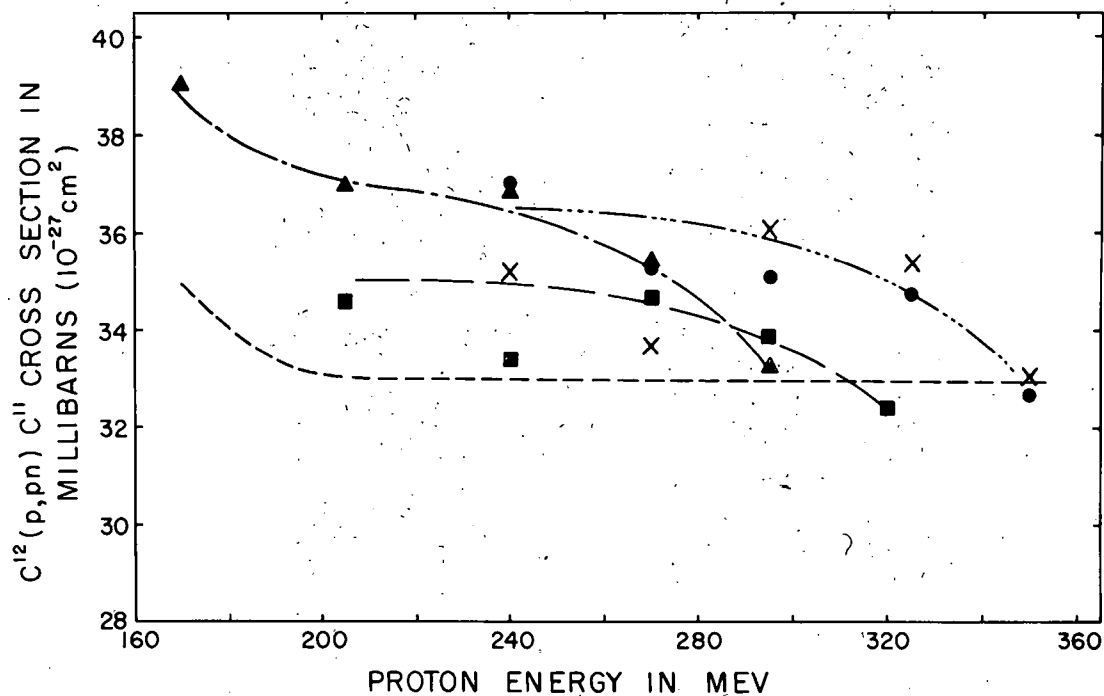


Fig. 3 The variation of the $C^{12}(p, pn) C^{11}$ cross section is shown as a function of proton energy. The dots and crosses represent measurements made with an incident proton energy of 350 Mev; the squares, with an incident proton energy of 320 Mev; and the triangles, with an incident proton energy of 295 Mev. The curves are drawn as a visual aid only. The short dashed line represents what is believed to be the actual variation of the cross section with energy in this region; the variation shown by the groups of points is believed to be a result of the method of measurement.

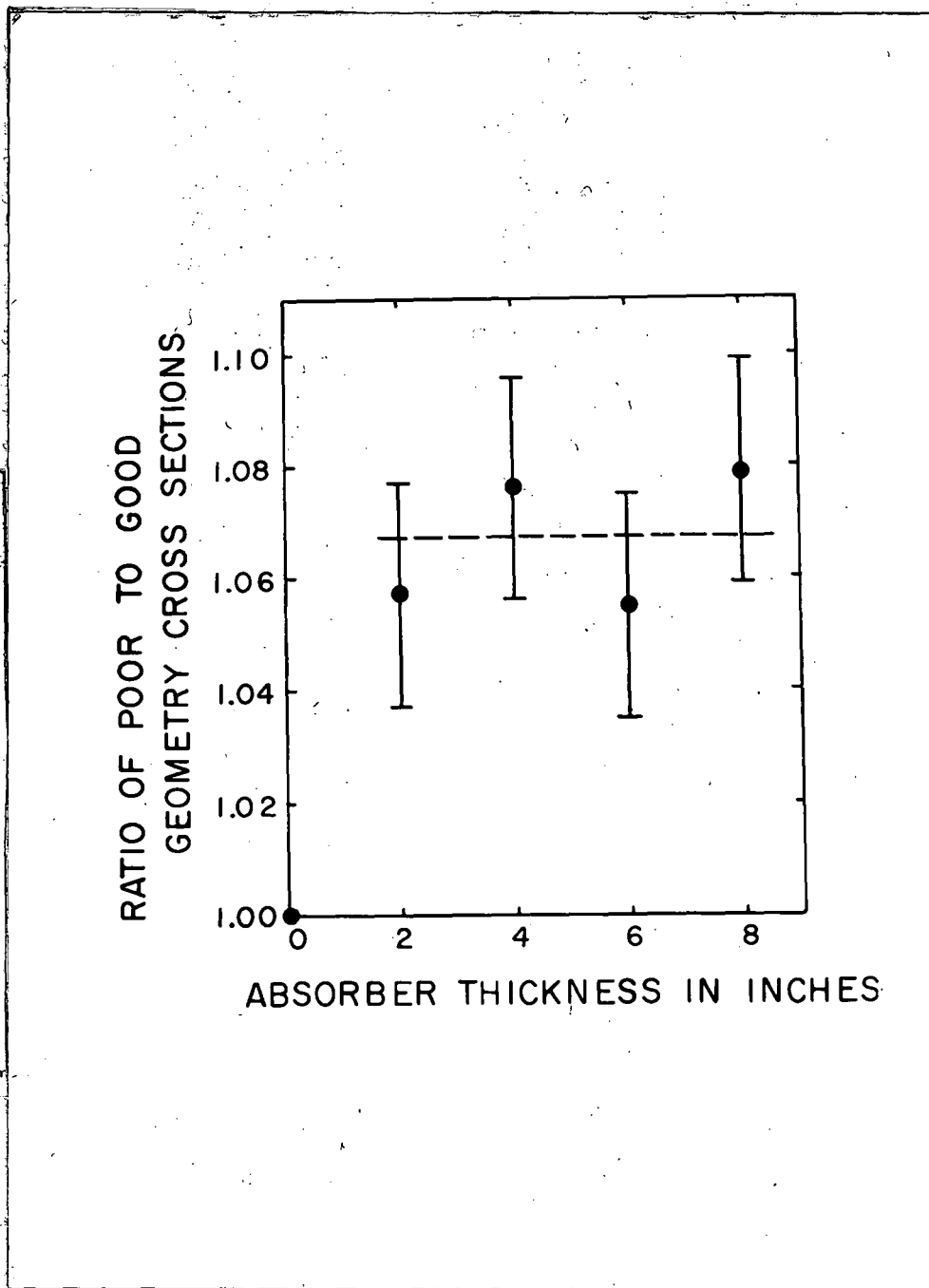


Fig. 4 The ratio of $C^{12}(p, pn)C^{11}$ cross sections determined by "poor" and "good geometry" methods of energy degradation (see text) as a function of absorber thickness. The dashed line is the mean of the four points shown and is the value used to correct all "poor geometry" measurements.

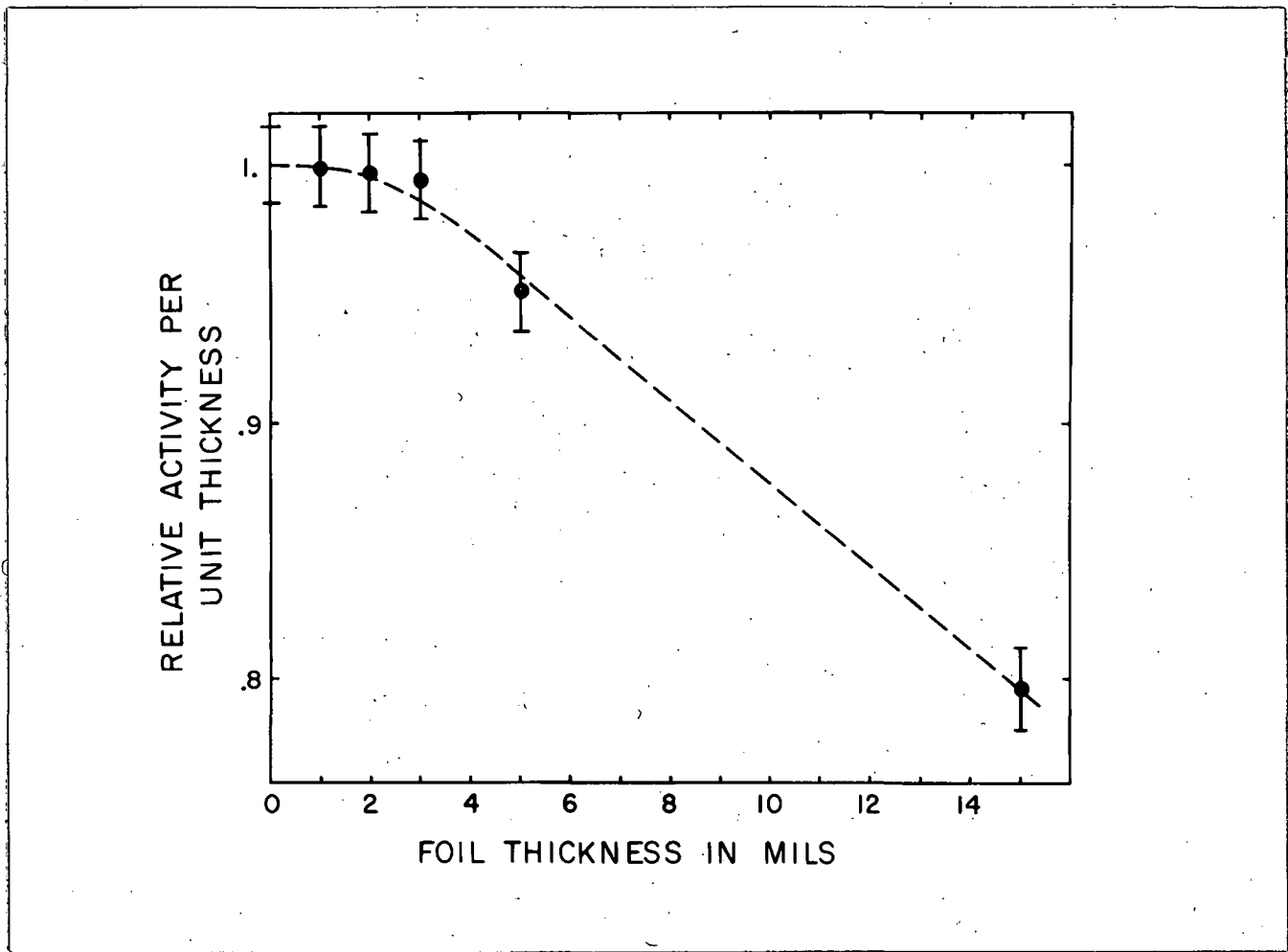


Fig. 5 The relative counting rate for C^{11} from the $C^{12}(p, pn)C^{11}$ reaction is plotted against foil thickness. The extrapolation to zero foil thickness is empirical and the adopted uncertainty in the estimated intercept is indicated in the figure.

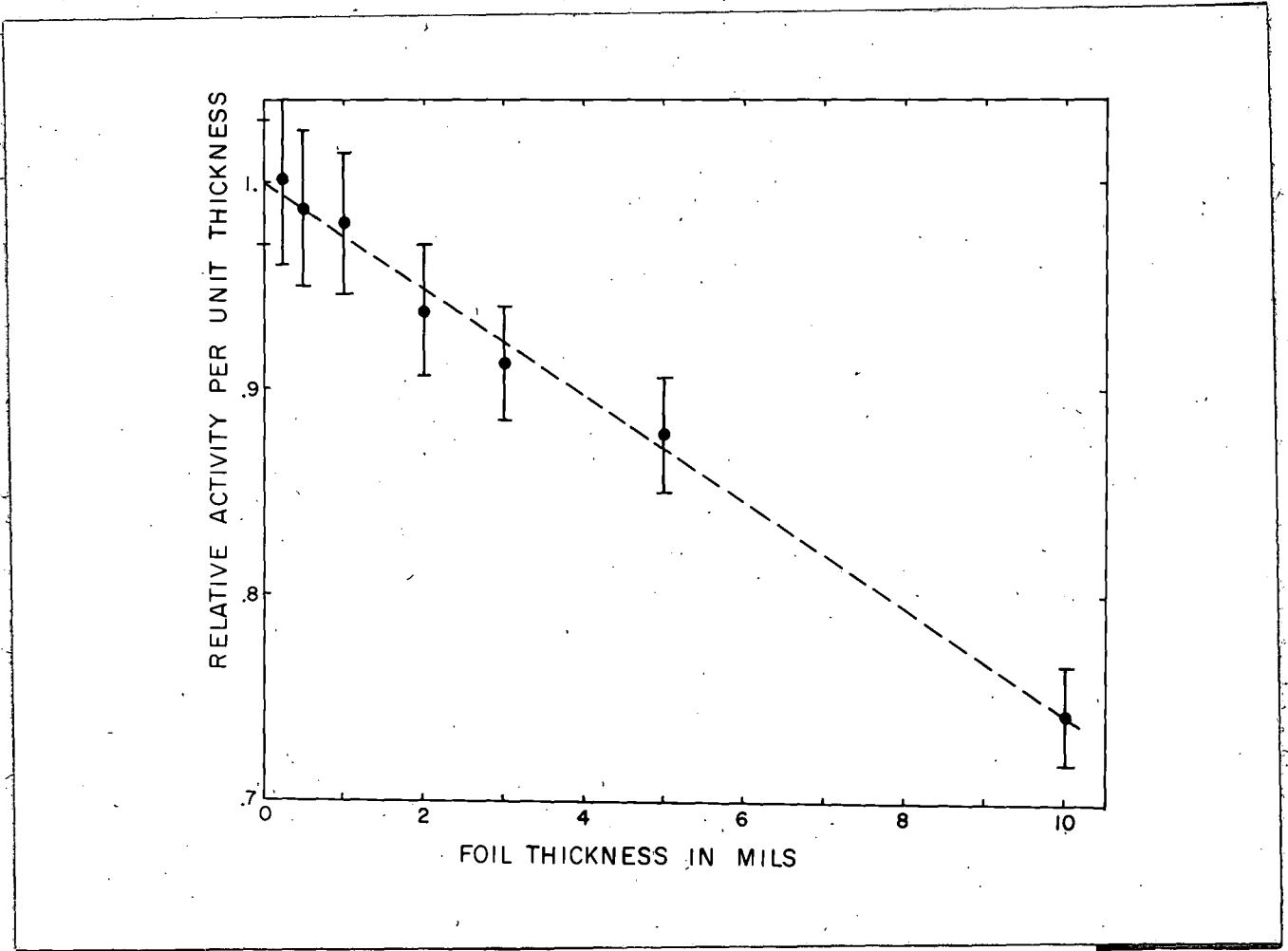


Fig. 6 The relative counting rate per unit thickness for Na^{24} from the $\text{Al}^{27} (n, \alpha) \text{Na}^{24}$ reaction is plotted against foil thickness. The extrapolation to zero foil thickness is empirical and the adopted uncertainty in the estimated intercept is indicated in the figure.

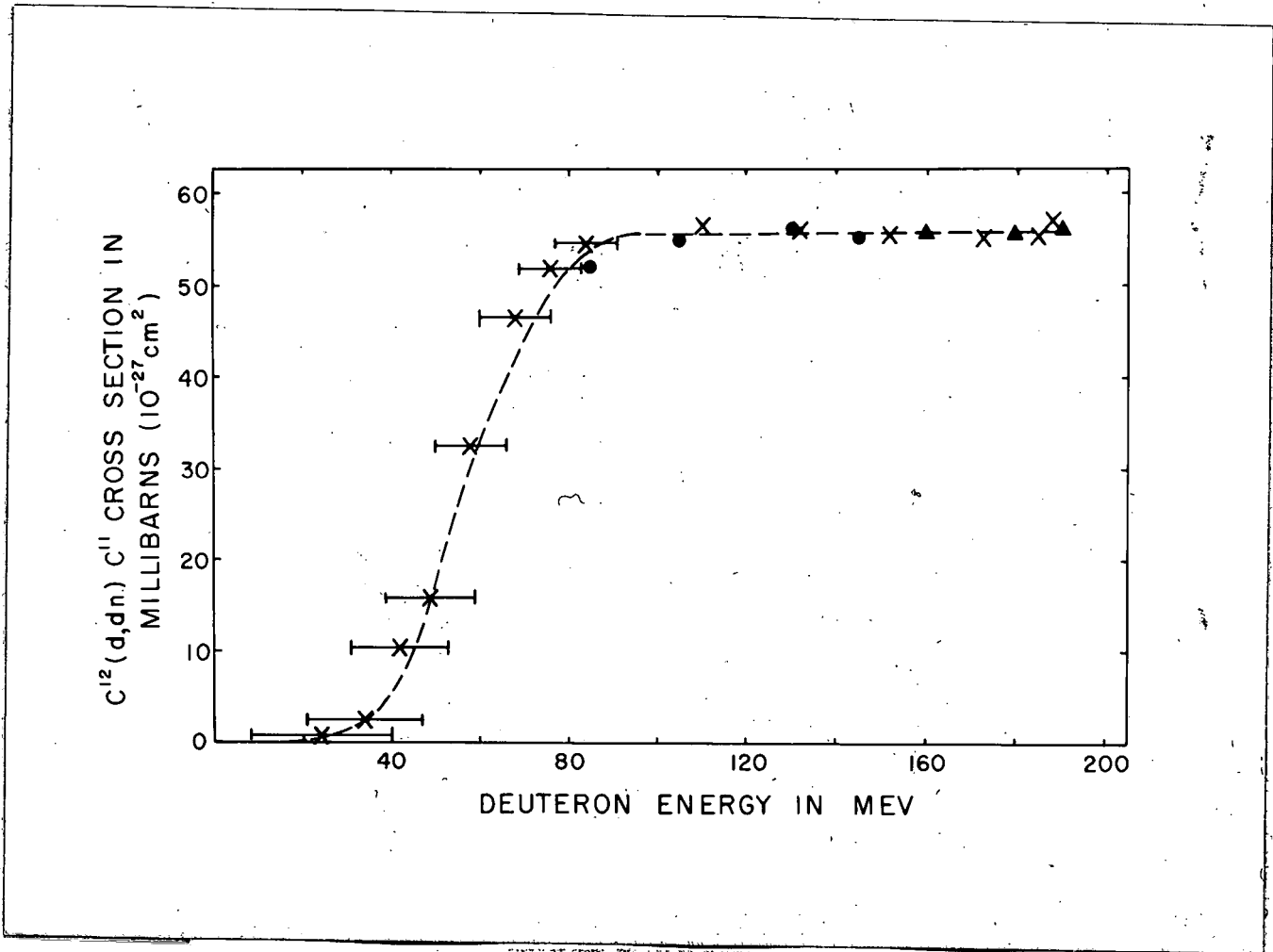
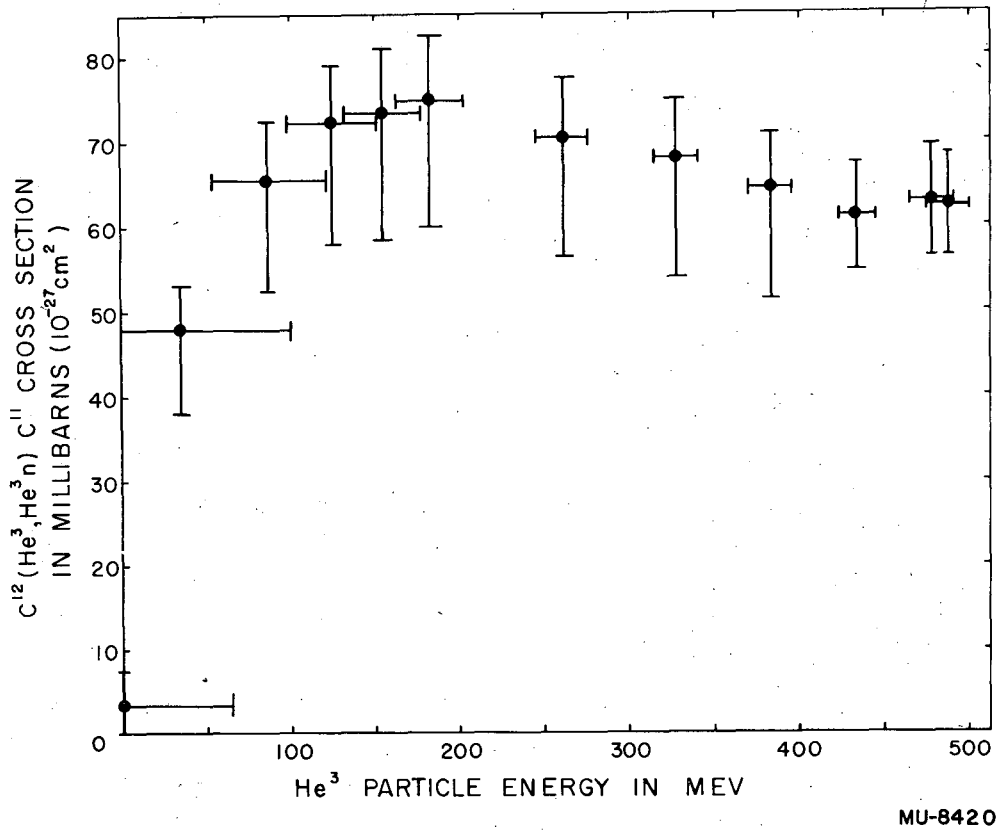


Fig. 7 The excitation function for the $C^{12}(d, dn)C^{11}$ reaction is plotted as a function of the deuteron energy. The triangles are "good geometry" measurements, and the dots are "poor geometry" measurements corrected as described in the text. The crosses are the end-window counter data normalized at 190 Mev to the other data. The positions of the low-energy points are uncertain to the extent of the horizontal lines, and in addition there is a spread of energies because of range straggling in the absorber.



MU-8420

Fig. 8 The excitation function for the $Cl^{12}(He^3, He^3n)Cl^{11}$ reaction is shown as determined from the end-window counter data. The placement of the low-energy points is uncertain to the extent indicated, and in addition there is a spread of energies due to range straggling. The correction for secondary-particle effects at less than maximum energy is very uncertain and is reflected in the unsymmetrical errors; no indicated trend in the excitation function can be separated from the large experimental uncertainties.